

Projection based whole body motion planning for legged robots

Diego Pardo, Michael Neunert, Alexander W. Winkler and Jonas Buchli

Abstract—In this paper we present a new approach for dynamic motion planning for legged robots. We formulate a trajectory optimization problem based on a compact form of the robot dynamics. Such a form is obtained by projecting the rigid body dynamics onto the null space of the Constraint Jacobian. As consequence of the projection, contact forces are removed from the model but their effects are still taken into account. This approach allows to solve the optimal control problem of a floating base constrained multibody system while avoiding the use of an explicit contact model. We use direct transcription to numerically solve the optimization. As the contact forces are not part of the decision variables the size of the resultant discrete mathematical program is reduced and therefore solutions can be obtained in a tractable time. Using a predefined sequence of contact configurations (phases), our approach solves motions where contact switches occur. Transitions between phases are automatically resolved without using a model for switching dynamics. We present results on a hydraulic quadruped robot (HyQ), including single phase (standing, crouching) as well as multiple phase (rearing, diagonal leg balancing and stepping) dynamic motions.

I. INTRODUCTION

Motor skills on state of the art legged robots are still far from mature, as they clearly do not move as smoothly and efficiently as animals yet. Regardless of specific and carefully designed implementations, there is no general approach for the online planning and execution of dynamic whole body motions on legged robots. In such systems, using hand designed or motion captured references tends to produce inefficient and artificial results.

Other approaches [18] use the well known Zero Moment Point (ZMP) [8] to maintain balance during motions. The typical simplified model used to calculate the ZMP for a legged robot is the cart-table model, which does not capture the full rigid body dynamics of the physical robot and can lead to instability. Additionally, the quasi-static stability criterion requires to keep the ZMP inside the support polygon created by the legs in contact. While this approach works well in practice, it is based on several assumptions, hindering dynamic and more natural looking motions which would be feasible from a physics perspective.

On the other hand, whole body motion planning and control based on optimization is demonstrating to be a very promising approach [3], [12], [9], [10]. It is clear that contact

forces play a decisive role in the resultant behavior of the robot, and therefore they need to be taken into account during the planning process. Trajectory optimization offers a framework where contact forces can be consistently included as decision variables. However, a continuous optimal control problem for floating base robots subject to kinematic constraints is so often too complex for analytical approaches and therefore numerical methods must be used. The choice of numerical technique has a significant influence on the computational effort and feasibility of the solution.

Numerical methods for trajectory optimization can be roughly classified as shooting or direct methods and both approaches have been applied to create dynamic motions for legged robots. In essence, all methods search for a set of decision variables (e.g., joint torques and external forces) such that a cost function is minimized while satisfying a set of constraints (e.g., system dynamics and kinematic constraints). The minimization is accomplished by iteratively following a numerical approximation of a gradient.

Broadly speaking, *shooting methods* obtain the data required for the gradient approximation by forward simulating the system dynamics and computing the resulting cost function. Importantly, these methods need to include the constraints as penalty terms in the cost function, i.e. adding the requisite of dynamic feasibility as a soft constraint. As a consequence, these methods may provide suboptimal solutions or even violate system dynamics. Most of the results have been verified in animation [10], i.e., playing back the state trajectories instead of forward integrating the equations of motion or applying the planned torques on a robot. To the best of our knowledge, there are no reports of experiments on torque control legged robots using shooting methods.

On the other hand, *direct methods* discretize the state, control and force trajectories over time and an optimization problem is stated over the values of the variables at the discretization points or nodes [12], [3]. The resulting problem can then be solved by a nonlinear programming (NLP) solver. One of the main advantages of direct methods is that constraints are enforced by the solver. This feature facilitates applying solutions to real robots, for instance adding bounds on the state and control variables.

As a consequence of discretizing both state and control, the dynamics of the system have to be verified in between the nodes, which increases the number of constraints. The large size of the subsequent discrete optimization is an important challenge, making direct methods computationally expensive and preventing its use for online motion generation. This fact is accentuated by including the contact forces as decision

This research has been funded through a Swiss National Science Foundation Professorship award to Jonas Buchli and by the Swiss National Centre of Competence in Research Robotics (NCCR Robotics) - Diego Pardo {depardo@ethz.ch}, Michael Neunert {neunertm@ethz.ch}, Alexander Winkler {winklera@ethz.ch} and Jonas Buchli {buchli.j@ethz.ch} are with the Agile & Dexterous Robotics Lab at the Institute of Robotics and Intelligent Systems, ETHZ Zürich, Switzerland.

variables. In [3] the use of the simpler, yet completely valid, centroidal dynamics of the robot was proposed to overcome this difficulty. The length of the problem is then reduced with respect to the one using the full model. Nevertheless, using the centroidal dynamics prevents the use of constraints or costs based on the joint torques, moreover additional kinematic constraints are required to obtain feasible solutions.

Another technique known as multiple shooting combines the shooting and direct approaches. Multiple shooting has been used for human-like whole body optimal control [15] and to the analysis of specific motion problems on humanoids [9]. Similar to direct methods, constraints can be explicitly formulated. As in shooting methods, however, this approach needs an explicit model for the contact dynamics to describe the changes between contact configurations or phases.

In this paper we present a new approach for whole body motion planning based on a direct method. Here we use a reduced version of the full body dynamics obtained from the projection of the equations of motion into the tangent space with respect to the constrained manifold. As a consequence of the projection, contact forces are removed from the dynamics whereas its effects are still taken into account. The main contribution of this paper is the integration of a direct transcription method for trajectory optimization with a model representing the direct dynamics of a legged robot where contact forces are not explicit. The projection of the equations of motion is obtained via an algebraic operator that depends only on kinematic quantities and thus obtaining solutions in a tractable time. Moreover, compared with shooting methods, our approach does not required an explicit contact model, reducing the complexity of the numerical optimization process.

This paper is organized as follows. Section II presents the optimal control problem of legged robots in a very general form and describes our solution approach. Section III reviews the main concepts of the projection of the equations of motion into a constraint space. In Section IV we describe the direct transcription method to generate motions in legged robots based on the projected model. Results are described in section V. Finally, conclusions and future work are discussed in section VI.

II. GENERAL FRAMEWORK

In general, the system dynamics of a robot can be modelled by a set of nonlinear differential equations,

$$\dot{\mathbf{x}}(t) = f(\mathbf{x}(t), \mathbf{u}(t)), \quad (1)$$

where $\mathbf{x} \in \mathbb{R}^{n_x}$ represents the system states and $\mathbf{u} \in \mathbb{R}^{n_u}$ the vector of inputs. The transition function $f(\cdot)$ defines the system evolution over time. Legged robots can be modeled as underactuated, floating base systems, i.e., the state space is given by $\mathbf{x} = [\mathbf{q}^T, \dot{\mathbf{q}}^T]^T$ where the generalized coordinate $\mathbf{q} = [\mathbf{q}_b^T, \mathbf{q}_r^T]^T$ includes base positions and orientations ($\mathbf{q}_b \in \mathbb{R}^6$) as well as joint configurations ($\mathbf{q}_r \in \mathbb{R}^n$), i.e., $n_x = 2 \times (6 + n)$. Control inputs are usually joint torques $\mathbf{u} = \boldsymbol{\tau} \in \mathbb{R}^n$.

In a very general formulation, a trajectory optimization problem for whole body motion planning and control in legged robots,

$$\begin{aligned} \min_{\mathbf{u}(t), \mathbf{x}(t)} \quad & J = \Psi(\mathbf{x}(t_f)) + \int_0^{t_f} \psi(\mathbf{x}(t), \mathbf{u}(t), t) dt \\ \text{s.t.,} \quad & \dot{\mathbf{x}} = f(\mathbf{x}, \mathbf{u}) \\ & \mathbf{g}_{0,l} \leq \mathbf{g}_0(\mathbf{x}(t_0), \mathbf{u}(t_0), t_0) \leq \mathbf{g}_{0,u} \\ & \mathbf{g}_{f,l} \leq \mathbf{g}_f(\mathbf{x}(t_f), \mathbf{u}(t_f), t_f) \leq \mathbf{g}_{f,u} \\ & \phi_l \leq \phi(\mathbf{x}(t), \mathbf{u}(t), t) \leq \phi_u \\ & \mathbf{x}_{min} \leq \mathbf{x}(t) \leq \mathbf{x}_{max} \quad \mathbf{u}_{min} \leq \mathbf{u}(t) \leq \mathbf{u}_{max} \end{aligned} \quad (2)$$

consists in finding a finite-time state and input trajectory $\mathbf{x}(t), \mathbf{u}(t), \forall t \in [0, t_f]$, such that a given criteria J is minimized, subject to a set of constraints. Intermediate $\psi(\cdot)$ and final $\Psi(\cdot)$ costs encode the objective of the task through J . The optimization is subject to the dynamics of the system, as well as to boundary conditions, $\mathbf{g}(\cdot)$, path constraints $\phi(\cdot)$, and simple bounds on the state and control variables.

The complexity of this optimization problem stems from the complexity of the dynamics of a legged robot. Besides the underactuation, legged robots are constantly establishing and breaking contacts with the environment adding constraints to its motion and generating ground reaction forces.

In [1], a method to derive direct dynamics of constrained mechanical systems based on the notion of a projector operator is presented. Constraint reaction forces are eliminated by projecting the original dynamics equations into the tangent space with respect to the constraint manifold. Moreover, the equations of motions are derived in a form that explicitly relates the generalized input force to the acceleration. The following section revisits the derivation of the constraint-consistent dynamics, describing those concepts relevant to understand our approach for planning in such a subspace.

III. DIRECT DYNAMICS OF A LEGGED ROBOT

In general, the dynamics of a legged robot can be modeled as a constrained multibody system, i.e.,

$$\mathbf{M}(\mathbf{q})\ddot{\mathbf{q}} + \mathbf{h}(\mathbf{q}, \dot{\mathbf{q}}) = \mathbf{S}^T \boldsymbol{\tau} + \mathbf{F}_c \quad (3)$$

subject to m kinematic constraints,

$$\Phi(\mathbf{q}) = \mathbf{0}. \quad (4)$$

where $\mathbf{M} \in \mathbb{R}^{(n+6) \times (n+6)}$ represents the inertia matrix, $\mathbf{h} \in \mathbb{R}^{n+6}$ is a generalized force vector, gathering Gravitational, friction, Coriolis and centrifugal effects. $\boldsymbol{\tau} \in \mathbb{R}^n$ is the vector of joint torques and $\mathbf{S} \in \mathbb{R}^{n \times (n+6)}$ is the joint selection matrix that reflects the underactuation. $\mathbf{F}_c \in \mathbb{R}^{n+6}$, represents the generalized constraint force acting on the robot DOF.

The set of constraints described in (4) models that there are certain points, c_j , of the robot which motion is instantaneously constrained, and their velocity is zero, i.e.,

$$\mathbf{J}_c \dot{\mathbf{q}} = \mathbf{0} \quad (5)$$

where $\mathbf{J}_c = \partial\Phi/\partial\mathbf{q} \in \mathbb{R}^{m \times (n+6)}$ is the Jacobian of the constraints with respect to the generalized coordinate. This can be used to express the generalized constraint force,

$$\mathbf{F}_c = \mathbf{J}_c^T \lambda \quad (6)$$

where $\lambda \in \mathbb{R}^m$ are the so-called Lagrange multipliers of the constraints. Notice that no assumption has been made on the rank of (4), and it may contain redundancies. For instance, in case of a point feet quadruped robot with all feet in contact with the ground, $\lambda \in \mathbb{R}^{12}$ represents the ground reaction forces on the feet, hence the constraints in (4) are redundant and $\Phi(\mathbf{q})$ is not full rank.

As first suggested in [1], constraint forces can be eliminated from (3) by projecting the dynamics onto the null space of \mathbf{J}_c , i.e., onto the tangent space with respect to the constrained manifold. Provided an orthogonal projection operator \mathbf{P} such that its range is equal to the null space of the Jacobian, i.e., $\mathcal{R}(\mathbf{P}) = \mathcal{N}(\mathbf{J}_c)$, it can be shown that such operator is an annihilator for the generalized constraint force¹, i.e., $\mathbf{P}\mathbf{F}_c = 0$. Applying the orthogonal operator to (3), the projected inverse dynamics of a constrained multibody system is then expressed in a descriptive form by,

$$\mathbf{P}\mathbf{M}\ddot{\mathbf{q}} = \mathbf{P}(\mathbf{S}^T \boldsymbol{\tau} - \mathbf{h}) \quad (7)$$

This equation could already be used as a constraint for the optimization, as it does not include the contact forces and the complexity of the original problem would be reduced. However, this expression does not consider the components of the null space orthogonal to the acceleration, i.e., the component of acceleration produced exclusively by the constraint and not by dynamics. The velocity constraint in (5) implies that the null space orthogonal component of the velocity must be equal to zero.

$$\dot{\mathbf{q}}_{\perp} = (\mathbf{I} - \mathbf{P})\dot{\mathbf{q}} = 0. \quad (8)$$

Differentiating (8) with respect to time, it can be seen that the null space orthogonal component of the acceleration ($\ddot{\mathbf{q}}_{\perp}$) is not necessarily equal to zero,

$$\ddot{\mathbf{q}}_{\perp} = (\mathbf{I} - \mathbf{P})\ddot{\mathbf{q}} = \mathbf{C}\dot{\mathbf{q}} \quad (9)$$

where $\mathbf{C} = d\mathbf{P}/dt$. Aghili proposed in [1] that combining (7) and (9), and assuming a square projector matrix $\mathbf{P} \in \mathbb{R}^{(n+6) \times (n+6)}$, a complete equation of motion of the constrained mechanical system can be obtained,

$$\ddot{\mathbf{q}} = \mathbf{M}_c^{-1} (\mathbf{S}^T \boldsymbol{\tau} - \mathbf{h} + \mathbf{C}_c \dot{\mathbf{q}}) \quad (10)$$

where $\mathbf{C}_c = \mathbf{M}\mathbf{C}$, whereas $\mathbf{M}_c \in \mathbb{R}^{(n+6) \times (n+6)}$, the so-called *constraint inertia matrix*, is defined as,

$$\begin{aligned} \mathbf{M}_c &= \mathbf{M} + \tilde{\mathbf{M}} \\ \tilde{\mathbf{M}} &= \mathbf{P}\mathbf{M} - (\mathbf{P}\mathbf{M})^T. \end{aligned} \quad (11)$$

¹As shown in [1], giving that $\mathbf{F}_c \in \mathcal{R}(\mathbf{J}_c^T)$ and by virtue of the fundamental relationship between the range space and the null space orthogonal associated with a linear operator and its transpose, it can be shown that $\mathbf{F}_c \in \mathcal{N}(\mathbf{J}_c)^{\perp}$. Vectors can be expressed as the sum of orthogonal components, $\dot{\mathbf{q}} = \dot{\mathbf{q}}_{\parallel} \oplus \dot{\mathbf{q}}_{\perp}$. According to (5), $\dot{\mathbf{q}} \in \mathcal{N}(\mathbf{J}_c)$, and as $\dot{\mathbf{q}}_{\parallel} = \mathbf{P}\dot{\mathbf{q}}$, i.e., $\dot{\mathbf{q}}_{\parallel} \in \mathcal{N}(\mathbf{J}_c)$, therefore, $\dot{\mathbf{q}}_{\perp} = 0$.

The equation of motion in (10) is completely compatible with the trajectory optimization problem in (2) and with the direct transcription approach described in the next section. It is worth mentioning that, as shown in [1], there is no unique way of combining (7) and (9) to obtain (10). Although all forms are equivalent, some might have computational advantages over others. As demonstrated in [1], the constraint inertia matrix in (11) is positive definite but not necessarily symmetric.

Finally, it is important to remark that the derivation of (10) assumes a square projector. That is the case of the orthogonal projector proposed in [1], and used throughout this paper,

$$\mathbf{P} = \mathbf{I} - \mathbf{J}_c^+ \mathbf{J}_c \quad (12)$$

where \mathbf{J}_c^+ denotes the pseudoinverse of \mathbf{J}_c . Other forms of projector operators have been proposed in the context of inverse dynamics control of floating base robots [13]. Nevertheless, these are not square and therefore cannot be used to compute a direct dynamics expression compatible with the direct transcription approach used in this work.

IV. DIRECT TRANSCRIPTION

We use direct transcription [2], [7] to find a feasible motion plan. This method translates the continuous formulation in (2) into a mathematical optimization problem with a finite number of variables that can be solved using an Nonlinear Programming Solver (NLP).

The decision variables $\mathbf{y} \in \mathbb{R}^p$ of the transcription problem are the discrete values of the robot state and control trajectories sampled at certain points or nodes. The time between nodes ΔT is not necessarily constant and has been included in the set of decision variables, i.e., $\mathbf{y} = \{\mathbf{x}_k, \mathbf{u}_k, \Delta T_k\}$ for $k = 1, \dots, N$, where N represents the total number of nodes.

The resulting NLP is then formulated as follows,

$$\begin{aligned} \min_{\mathbf{y}} \quad & f_0(\mathbf{y}) \\ \text{s.t.,} \quad & \zeta(\mathbf{y}) = 0 \\ & \mathbf{b}_{min} \leq \mathbf{b}(\mathbf{y}) \leq \mathbf{b}_{max} \\ & \mathbf{y}_{min} \leq \mathbf{y} \leq \mathbf{y}_{max}, \end{aligned} \quad (13)$$

which contains a scalar and derivable objective function $f_0(\mathbf{y})$, a set of boundary and path constraints $\mathbf{b}(\cdot)$ and bounds $[\mathbf{y}_{min}, \mathbf{y}_{max}]$ on the state and control variables.

A. Dynamic constraints

The original set of differential equations representing the dynamics of the robot in (1) is replaced with a vector of dynamic constraints or *defects* $\zeta(\cdot) \in \mathbb{R}^{(N-1) \times n_x}$. Although there are different alternatives to formulate the dynamic constraints [11], [2], we use a trapezoidal approximation for the dynamics,

$$\zeta \doteq \mathbf{x}_{k+1} - \mathbf{x}_k - \frac{\Delta T}{2} [f(t_k) + f(t_{k+1})] = 0 \quad (14)$$

where the notation $f(t_i) = f(\mathbf{x}_i, \mathbf{u}_i)$ has been adopted for simplicity. Notice that the inverse dynamics in (7) cannot be used to compute this form of defect as $f(\cdot)$ cannot be computed through matrix inversion. On the other hand, the defects can be easily computed using (10).

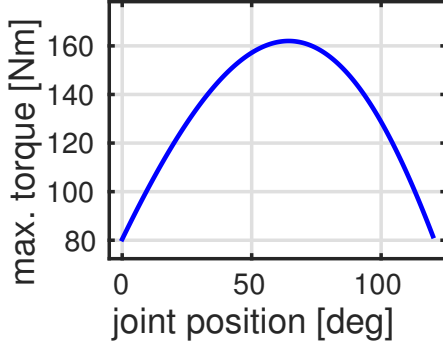


Fig. 1. Maximum torque of HyQ knee is function of the joint configuration due to a varying leverarm. This function is then used as path constraint to avoid limiting the capacities of the robot.

B. Torque bounds as path constraints

As in the case of hydraulically actuated robots, torque limits may depend on the configuration of the robot, i.e., $\tau_{max} = \varphi(\mathbf{q})$. For instance, Fig. 1 shows the maximum torque that can be applied at the knee joint of the hydraulically-actuated quadruped (HyQ) [16]. We have added path constraints allowing the robot to use the actual maximal torque available, and thus exploiting its dynamic capacities. The constraint can be transcribed for the value of the torque at each node as follows,

$$0 \leq \varphi_i(\mathbf{q}) - \tau_i \leq \infty \quad (15)$$

C. Contact Points and Kinematic constraints

It is important to add kinematic constraints to satisfy the assumption that points c_j are in contact, and therefore the projection is valid. In general, if \mathcal{S}_j groups the valid contact regions (floor, wall, etc), the contact point used to generate the projection (i.e., \mathbf{J}_c) should satisfy, $c_j \in \mathcal{S}_j$.

For instance, in the case of the quadruped robot used in this paper, contact points are in the feet and the valid contact region is the ground, therefore the contact point constraint can be expressed as,

$$f_{kin}^{c_j}(\mathbf{q}) = 0. \quad (16)$$

where $f_{kin}^{c_j} \in \mathbb{R}$ is the kinematic function providing the perpendicular distance from the foot to the ground.

In order to facilitate the numerical optimization, other kinematic constraints that enforce the assumptions made to derive the projected dynamics may be added. For instance, when the dynamic constraints are satisfied, those kinematic constraints in (5) and its derivative, i.e.,

$$\mathbf{J}\ddot{\mathbf{q}} - \dot{\mathbf{J}}\dot{\mathbf{q}} = 0, \quad (17)$$

are necessarily being satisfied. Adding this constraints is straightforward and we observed that this helps the solver in finding feasible solutions.

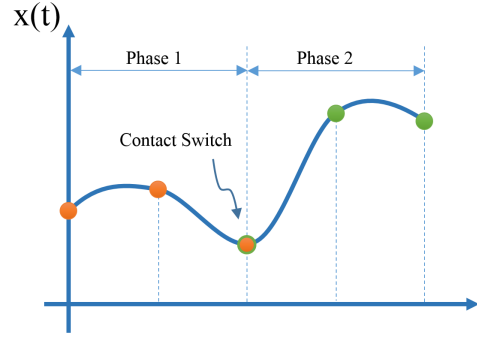


Fig. 2. The phases of the optimization are defined by the contact configuration of the robot. Transition between phases is handled automatically by the method, as dynamic constraints are verified in between the nodes. Last point of a phase also satisfy the dynamic constraint of the next phase.

D. Friction cone constraint

In order to generate feasible solutions, ground reaction forces at contact points $\lambda_j \in \mathbb{R}^3$ should be unilateral (i.e., the robot only can push to the ground) and its tangential component $\lambda_j^{x,y}$ should avoid sliding and maintain the contact, i.e., respecting the friction cone. This constraint can be written as,

$$-\infty \leq \|\lambda_j^{x,y}\| - \mu \cdot \lambda_j^z \leq 0 \quad (18)$$

where μ represents the friction coefficient between the contact point and the surface. This constraint already imposes the unilateral condition.

Even though contact forces are not part of the decision variables, it can be uniquely defined as a function of the state and control by an algebraic expression resulting from decoupling the dynamics, as derived in [13].

$$\lambda_i = \mathbf{R}^{-1} \mathbf{Q}_c^T (\mathbf{M} \cdot \mathbf{f}(t_i) + \mathbf{h} - \mathbf{S}^T \tau_i) \quad (19)$$

where \mathbf{Q}_c and \mathbf{R} derive from the QR decomposition of the constraint Jacobian $\mathbf{J}_c^T = \mathbf{Q}[\mathbf{R}^T \mathbf{0}]^T$, and, $\mathbf{Q} = [\mathbf{Q}_c \mathbf{Q}_u]$.

E. Switching contact configuration

Given that the dynamics are different for each contact configuration, the sequence of contacts defines different optimization *phases* [2]. The sequence of contact configuration has to be defined beforehand, while the duration of the phases is optimized over. Transitions between phases are handled automatically by the method, as constraints are verified in between nodes. At the transition nodes the trajectory satisfy the dynamics of both phases (see Fig. 2).

V. RESULTS

We have applied the framework described above to the generation of motions on the quadruped robot HyQ. This section describes the robot and shows the results obtained.

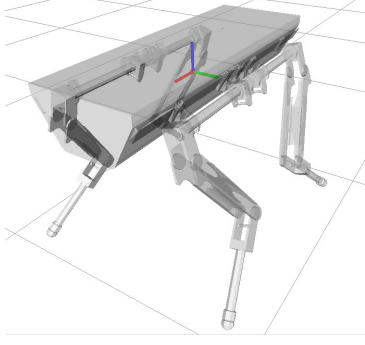


Fig. 3. Unified Robot Description Format (URDF) model of the Hydraulically-actuated Quadruped (HyQ). Dimensions at nominal configuration : 80cmx40cmx60cm. Each leg has 3DOF (hip abduction, hip flexion and Knee)

A. HyQ Robot and Conventions

Fig. 3 shows the HyQ robot. This robot is approximately 80cm long and 50cm wide, and it weights around 80Kg. Each leg has three DOF (HAA: Hip abduction/adduction, HFE: Hip flexion/extension and KFE: Knee flexion/extension - KFE) and it is fully torque controllable. Generating agile and dynamic motions in this type of robots is challenging due to its rigid body dynamics. At the same time the high bandwidth of hydraulic actuation offers an opportunity to exploit dynamic capabilities.

The equations of motion of the robot are based on the rigid body dynamics model provided by [5], on top of this we implemented the floating base dynamics using Plucker coordinates as suggested in [4], i.e., linear and angular velocities of the base are expressed in base coordinate frame, whereas position and orientation (XYZ Euler angles) are represented with respect to an inertial frame.

B. Feedback Stabilization

In order to effectively apply the solutions of the optimization to the robot, it is necessary to use a stabilizing feedback controller. We use a Time Variant Linear Quadratic Regulator (TVLQR) [17] around the optimized state and control trajectories $\mathbf{x}^*(t), \mathbf{u}^*(t)$. This controller provides optimal full state feedback gains $\mathbf{K}(t) \in \mathbb{R}^{n_u \times n_x}$. The total control applied to the robot, \mathbf{u}_T , amounts to

$$\mathbf{u}_T(t) = \mathbf{u}^*(t) + \mathbf{K}(t)(\mathbf{x}(t) - \mathbf{x}^*(t)).$$

Fig. 4 shows the trajectory of the 36 gains influencing the feedback control of a single torque command (e.g., Left Hind Knee) during a crouching motion. We use the projected dynamics for the linearization and subsequent solution of the differential Riccati equation.

C. Forward Integration and Simulation Environment

Optimized trajectories were initially tested performing the forward integration of (10). Nevertheless, this is a limited test as it does not include contact reaction forces and it assumes perfect sensor information of the pose of the robot body. Therefore, results were also validated in a simulation environment [14] with an independent contact and noise

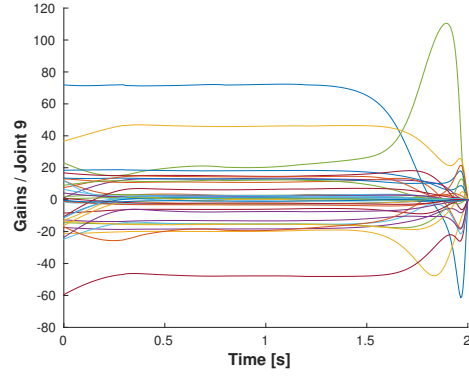


Fig. 4. Gains Trajectories obtained using TVLQR. Whole body feedback is implemented and therefore all the state errors affects the final torque applied to the joints. This plot shows the gains corresponding to the feedback torque of Joint 9 (Left Hind Knee) during *crouching* motion.

model. Finally, and in order to perform the validation under the most realistic conditions, the feedback of the state of the base was obtained using a state estimator.

D. Single Phase Motions

Motions with single contact configuration were generated in order to validate all the elements involved in the system. A quadratic cost function was used to obtain a *standing* behavior

$$J_{standing} = \bar{\mathbf{x}}^T \mathbf{Q}_s \bar{\mathbf{x}} + \bar{\mathbf{u}}^T \mathbf{R}_s \bar{\mathbf{u}} \quad (20)$$

where, $\bar{\mathbf{x}} = \mathbf{x} - \mathbf{x}_{nom}$ and $\bar{\mathbf{u}} = \mathbf{u} - \mathbf{u}_{nom}$ are the difference of the state and control with respect to their nominal values. Nominal joint configuration for the standing behavior is shown in Fig. 3. The base coordinate system and the inertia coordinate system are aligned at the beginning of the motion, therefore the initial robot pose is given by $\mathbf{q}_b = [\mathbf{0}_{1 \times 3} \ \mathbf{0}_{1 \times 3}]^T$. Fig. 5 shows the control signals found for the optimization problem using $N = 6$ discretization points for a $T = 2s$ trajectory. The contact constraint in (17) is verified by the signals in Fig. 6. Results of the simulation are shown in Fig. 7. These results confirm that control trajectories obtained using the projected dynamics are consistent with the dynamics of the robot since the complete system follows the plan even though the simulation includes contact forces and noise.

Modifying the nominal posture and cost corresponding to the z component of the position of the base, the system finds trajectories and controls to crouch down to the desired position. Fig. 8 shows the signals obtained during simulation.

E. Multiphase Motions

In order to generate more elaborated and dynamic motions, different sequences of contact configurations were used. Fig 12 shows the final configuration corresponding to the intermediate phase of different motions (rearing, diagonal legs balancing and stepping). All motions start with the same initial nominal posture and contact configuration.

The simulations described in this section are shown in the video attached to this paper: https://youtu.be/_fy-E40evjE

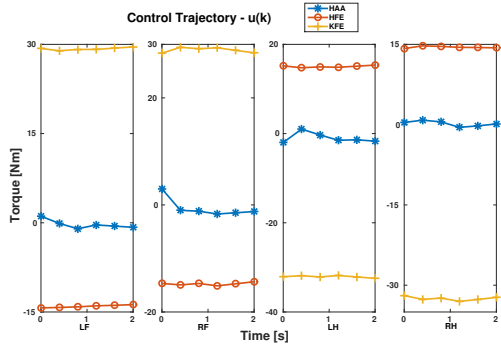


Fig. 5. Output of the trajectory optimization for the *standing* example. Three torques trajectories per leg are shown : HAA (blue star), HFE (yellow plus) and KFE (red circles)

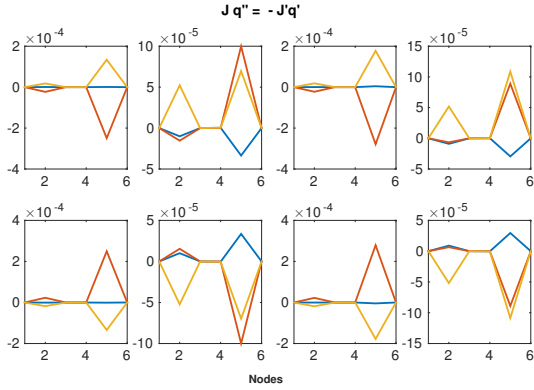


Fig. 6. The first row of plots correspond to the term $\mathbf{J}\ddot{\mathbf{q}}$, for each leg at the discretization nodes. The second row correspond to the term $\ddot{\mathbf{J}}\dot{\mathbf{q}}$. It can be observed that the second derivative of the kinematic constraints is satisfied.

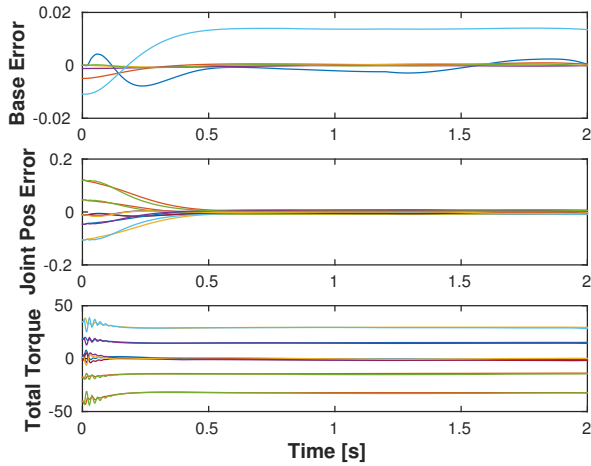


Fig. 7. Simulation of a single phase motion with all feet on the ground. The cost function used for this motion penalizes any motion of the base, as a result, the robot stays standing. The plots shown here are intended to demonstrate the overall behavior of the robot during this task. Top : Base position and orientation error, stays bounded and near the origin. Middle : Joint position error of all joints converge to zero. Bottom: Torque commands are very low and the feedback component absorbs numerical integration errors as well as compensation for the effects of the contact model.

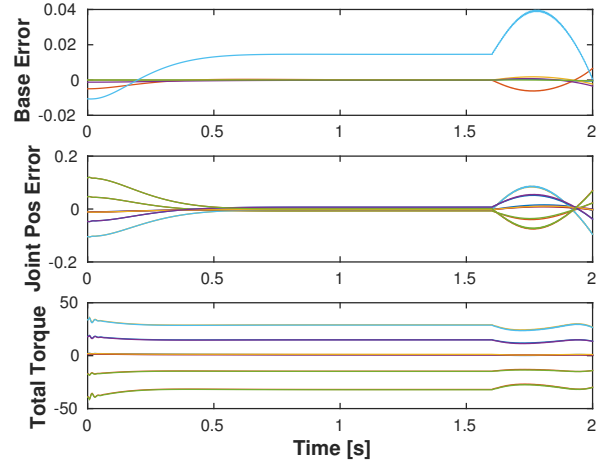


Fig. 8. Simulation of a *crouching* motion. Changing the cost and nominal value corresponding to the vertical component of the position of the base, the system generates trajectories for the states and controls in order to move the robot towards the desired position. Description of the plots is similar to the one used in Fig. 7

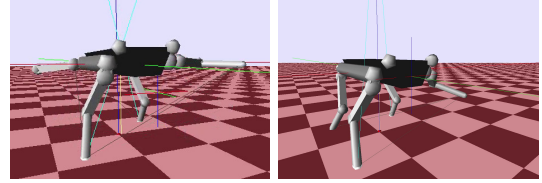


Fig. 9. Balancing

Fig. 10. Stepping

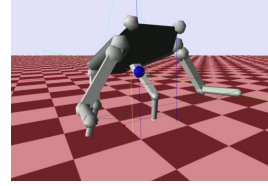


Fig. 11. Rearing

Fig. 12. Images captured in SL Simulation environment [14]. Final configuration corresponding to different multiphase motions (Stepping, Rearing, diagonal legs balancing).

F. Comparison with centroidal dynamics

All motions presented were obtained by the proposed optimization in few minutes of processing in a common laptop. However, this is not a valid measure of performance as too many elements of the implementation are accountable to be optimized. In order to understand the impact of our contribution, here we present a rough analysis of the size of the problem compared with the state of the art on whole body motion planning using direct transcription methods [3].

Table I shows the total number of decision variables and constraints (per node) required in order to solve a single phase motion on the HyQ robot (four feet on the ground)². It can be seen that the complexity of the problem is reduced using the projected dynamics and thus it can be hypothesized that the computational time required to solve the problem under same implementation is less.

²As described in Section II-D of [3]

TABLE I

NUMBER OF DECISION VARIABLES AND CONSTRAINTS (PER NODE) FOR A SINGLE PHASE MOTION ON HYQ (ALL FEET IN CONTACT)

| Method | Decision Variables | Constraints |
|---------------------|--------------------|-------------|
| Centroidal Dynamics | 76 | 63 |
| Projection | 49 | 48 |

G. Software Implementation

Our system is developed in C++, based on the Eigen library for vector manipulation and linear algebra. Given an implementation of the equation of motion of the legged robot and a sequence of contact configurations, our systems automatically projects the dynamics and generates the corresponding numerical optimization problem. The system provides an interface to well known SNOPT [6] solver, used to obtain the results presented in this paper.

VI. CONCLUSIONS AND FUTURE WORK

The projection of the dynamics onto the null space of the Jacobians of its constraints allows to reduce the complexity of the model, facilitating the use of direct methods for trajectory optimization. The motions generated for the hydraulically-actuated robot satisfy the kinematic constraints in (5) and (17) even if they are not explicitly added to the optimization problem, demonstrating the consistency of the formulation. Motions including switching contacts (2 phases), have been shown to demonstrate the feasibility of the method.

Single phase motions were straightforward to implement in the real robot, however, we have observed that results tend to be at the limit of dynamic stability, and therefore they are very sensitive to modelling errors and noise. It seems that optimality of the solutions stress their feasibility (in the real robot). Development of robust feedback controllers is required to achieve the actual exploitation of the dynamics proposed by optimization approaches as the one presented in this paper.

REFERENCES

- [1] Farhad Aghili. A unified approach for inverse and direct dynamics of constrained multibody systems based on linear projection operator: applications to control and simulation. *Robotics, IEEE Transactions on*, 21(5):834–849, Oct 2005.
- [2] John T. Betts. Survey of numerical methods for trajectory optimization. *Journal of Guidance, Control, and Dynamics*, 21(2):193–207, 1998.
- [3] Hongkai Dai, Andres Valenzuela, and Russ Tedrake. Whole-body motion planning with centroidal dynamics and full kinematics. In *IEEE-RAS International Conference on Humanoids Robots*, 2014.
- [4] Roy Featherstone. *Rigid Body Dynamics Algorithms*. Springer-Verlag New York, Inc., Secaucus, NJ, USA, 2007.
- [5] M. Frigerio, J. Buchli, and D.G. Caldwell. Code generation of algebraic quantities for robot controllers. In *Intelligent Robots and Systems (IROS), 2012 IEEE/RSJ International Conference on*, pages 2346–2351, Oct 2012.
- [6] P. Gill, W. Murray, and M. Saunders. SNOPT: An SQP algorithm for large-scale constrained optimization. *SIAM Review*, 47(1):99–131, 2005.
- [7] C. Hargraves and S. Paris. Direct trajectory optimization using nonlinear programming and collocation. *Journal of Guidance, Control, and Dynamics*, 10(4):338–342, 1987.
- [8] Shuji Kajita, Fumio Kanehiro, Kenji Kaneko, Kiyoshi Fujiwara, Kensuke Harada, Kazuhito Yokoi, and Hirohisa Hirukawa. Biped walking pattern generation by using preview control of zero-moment point. In *IEEE International Conference on Robotics and Automation*, pages 1620–1626, 2003.
- [9] K. H. Koch, K. Mombaur, P. Souères, and O. Stasse. Optimization based exploitation of the ankle elasticity of hrp-2 for overstepping large obstacles. In *International Conference on Humanoid Robots*, 2014.

- [10] I. Mordatch, E. Todorov, and Z. Popović. Discovery of complex behaviors through contact-invariant optimization. *ACM Trans. Graph.*, 31(4):43:1–43:8, July 2012.
- [11] D. Pardo, L. Moeller, M. Neunert, A. W. Winkler, and J. Buchli. Evaluating direct transcription and nonlinear optimization methods for robot motion planning. In *Arxiv Cornell University*, 2015.
- [12] Michael Posa, Cecilia Cantu, and Russ Tedrake. A direct method for trajectory optimization of rigid bodies through contact. *International Journal of Robotics Research*, 33(1):69–81, 2014.
- [13] L. Righetti, J. Buchli, M. Mistry, and S. Schaal. Inverse dynamics control of floating-base robots with external constraints: A unified view. In *Robotics and Automation (ICRA), 2011 IEEE International Conference on*, pages 1085–1090, 2011.
- [14] S. Schaal. The sl simulation and real-time control software package. Technical report, 2009.
- [15] G. Schultz and K. Mombaur. Modeling and optimal control of human-like running. *Mechatronics, IEEE/ASME Transactions on*, 15(5):783–792, 2010.
- [16] C Semini, N G Tsagarakis, E Guglielmino, M Focchi, F Cannella, and D G Caldwell. Design of HyQ – a hydraulically and electrically actuated quadruped robot. *Journal of Systems and Control Engineering*, 2011.
- [17] Russ Tedrake. Underactuated robotics: Algorithms for walking, running, swimming, flying, and manipulation (course notes for mit 6.832), Downloaded in Fall, 2014.
- [18] A. W. Winkler, C. Mastalli, I. Havoutis, M. Focchi, D. Caldwell, and C. Semini. Planning and Execution of Dynamic Whole-Body Locomotion for a Hydraulic Quadruped on Challenging Terrain. In *IEEE International Conference on Robotics and Automation*, 2015.